Normal Radiographic and Xeroradiographic Anatomy of the Bovine Manus

M. J. Shively, *D.V.M., M.S., Ph.D.*
J. E. Smallwood, *D.V.M., M.S.*
College of Veterinary Medicine
Texas A & M University
College Station, Texas 77843

Historically food animal medicine has been limited to some degree by economic factors which often dictate simplified diagnostic procedures and treatments. As a consequence, practitioners in this area have frequently been forced to rely more heavily on the "art" of medicine. Their colleagues in companion animal practice, however, have more often enjoyed the comparative economic freedom stemming from the emotional bond between client and patient. As a result, the "Science" aspect of veterinary medicine has advanced more rapidly in companion animal practice, and numerous types of technology which have been routinely used in this area are just beginning to be fully employed in the food animal field.

Radiography is an example. Rarely used in food animal medicine barely a decade ago, it has now become an integral part of progressive food animal practice. This is the cumulative result of a number of factors. First, the general advancement of radiographic technology has made better portable units available. Second, some "pets" and breeding animals are valued considerably higher by their owners than their market worth. Finally, the use of artificial insemination with semen preservation and extension has markedly increased the value of many male breeding animals and the advent of ova transfer techniques has similarly increased the value of prized females.

Herein are illustrations of the major radiographic features of the bovine manus. The five standard views normally used to radiographically examine the equine carpus are presented, as well as dorsopalmar (A.P.) and oblique views of the digits. A lateral projection of the digits is not included because the unavoidable superimposition which occurs on mediolateral or lateromedial views makes interpretation of the resulting films somewhat difficult.

Xeroradiographs representing the same views as the conventional radiographs are presented to compare the imaging quality of the two techniques. Xeroradiography differs from conventional radiography in several respects. Instead of radiographic film which is wet-processed, xeroradiography is a completely dry process. It uses a selenium-coated aluminum plate which is electrostatically charged in a "conditioner" unit. This unit automatically inserts the plate into a plastic cassette which is then exposed using a conventional X-ray machine. The electrostatic charges on the selenium-coated plate are rearranged during the exposure to form a latent image of the subject composed of varying charge densities. After exposure, the cassette is placed in a "processor" unit which automatically opens the cassette and subjects the charged plate to multiple bursts of a charged powder (toner). The charged toner particles are attracted to or repelled from specific areas on the plate according to the charge density of the latent image. This forms a visible image on the plate composed of varying amounts of the charged powder. This toner image is then transferred to a piece of plastic-coated paper by direct contact. The toner image is fused to the paper by heat to form a xeroradiograph which exits the processor unit ready for viewing and interpretation.

Xeroradiography has the advantages of excellent detail and imaging characteristics which allow simultaneous visualization of soft tissue and dense bone. However, it is more expensive than conventional radiography unless many exposures are made. In addition, a high KVP and mAs technique is required which results in greater exposure to the patient. Also, many practitioners may have X-ray machines incapable of producing the beam strength required.

The anatomic terminology conforms to the anglicized version of the 1973 edition of *Nomina Anatomica Veterinaria.* Some commonly used and/or obsolete synonyms are included in parentheses.

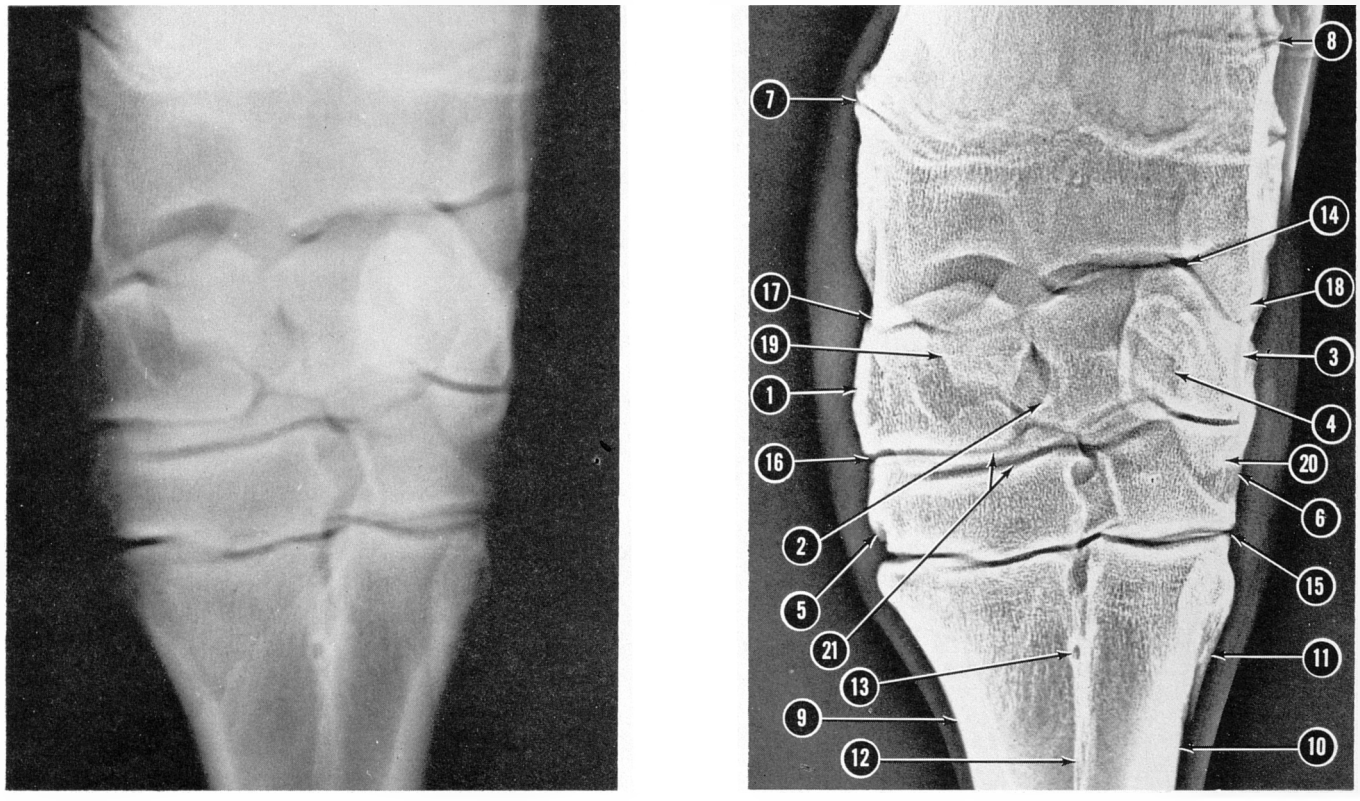

A. Radiograph *B. Xeroradiograph*

Figure 1

Dorsopalmar (AP) View of the Left Carpus

There are six carpal bones arranged in two rows in the carpus of domestic ruminants. In the proximal row are the medially-located radial carpal bone (1), the intermediate carpal bone (2), the superimposed ulnar carpal bone (3) and accessory carpal bone (4). The distal row includes the fused second and third carpal bones (C2+3) on the medial side (5) and the fourth carpal bone laterally (6). The first carpal bone is absent. The distal physes of the radius (7) and the ulna (8) separate the distal epiphyses of these bones from their respective diaphyses in this relatively young animal. The fused third (9) and fourth (10) metacarpal bones (Mc3+4) are the only weight-bearing metacarpal elements. The first two metacarpal bones are absent and the fifth metacarpal bone (Mc5) is reduced to a small vestige (11) which articulates with the proximal, lateral aspect of the fourth metacarpal bone. In the sheep Mc5 is often absent or is represented by a ridge on Mc3+4. The division between the third and fourth metacarpal bones remains obvious in the adult as the shallow dorsal and palmar longitudinal grooves (12) which are superimposed in this projection. These grooves are vascular impressions and are connected proximally and distally by the proximal metacarpal canal (13) and the distal metacarpal canal (Fig 6/4).

The carpal joint complex includes the antebrachiocarpal joint (14), the intercarpal joints, and the carpometacarpal joints (15). The antebrachiocarpal joint includes the larger radiocarpal joint and the smaller ulnocarpal joint within the same synovial capsule. The term "radiocarpal joint" is popularly (but incorrectly) used to refer to both of these subunits collectively. The intercarpal joints include the articulations between the individual carpal bones from side to side as well as proximally-distally. The collective intercarpal joints between the proximal and distal rows of carpal bones comprise the middle carpal joint (16). The synovial cavities of the middle carpal joint and the carpometacarpal joints communicate, but the antebrachiocarpal joint cavity is distinct and separate.

The difficulty encountered in interpreting carpal radiographs is related to superimpositions resulting from the irregular shapes of the carpal components. The styloid processes of the radius (17) and ulna (18) extend distally over the shadows of the radial and ulnar carpal bones respectively. The palmar aspect of the intermediate carpal bone (19) extends medially and is overshadowed by the radial carpal bone. Finally, the ulnar carpal bone has a palmar process (20) which is superimposed on the fourth carpal bone. The "double" joint space in the middle carpal joint (21) results from the fact that the articular surfaces are curved and is not due to obliquity of the X-ray beam. The "cleaner" appearance of the carpometacarpal joints (15) results from their nearly planar articular surfaces, whereas those of the antebrachiocarpal joint (14) are very curved and cause poor radiographic definition of the joint space.

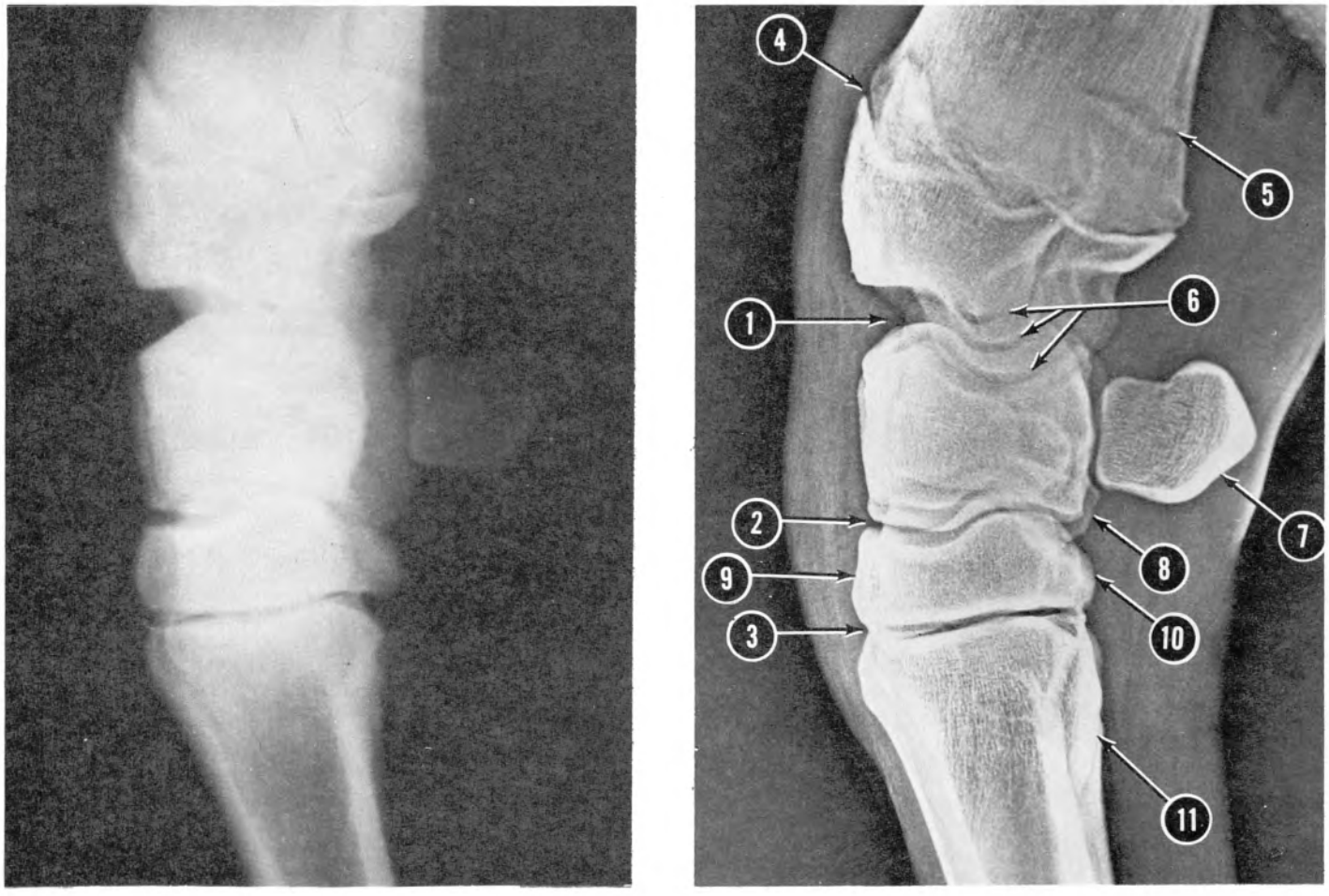

A. Radiograph *B. Xeroradiograph*

Figure 2

Lateromedial View of the Left Carpus

The antebrachiocarpal joint (1), middle carpal joint (2), and carpometacarpal joints (3) are readily distinguishable. The distal physis of the radius (4) is also easily observed but the distal physis of the ulna (5) is partially obscured by the superimposed radius. The various radiolucencies (6) in the antebrachiocarpal joint result from the tangential intersection of the X-ray beam with the irregular (non-planar) junction of the distal radiusulna and the proximal row of carpal bones. Note that the accessory carpal bone (7) articulates only with the ulnar carpal bone in contrast to most other domestic species in which it also articulates with the ulna. The palmar process of the ulnar carpal bone which extends distally is evident (8). In the distal row of carpal bones, C2+3 (9) projects further dorsally while the fourth carpal bone (10) extends further palmarly. This relationship is exaggerated by the slightly different perspective of the radiograph in comparison to the xeroradiograph. For the same reason the fifth metacarpal bone (11) is better isolated on the radiograph than on the xeroradiograph. The slight flexion of the antebrachiocarpal joint is due to the fact that the animal was not bearing weight on the limb when the exposures were made.

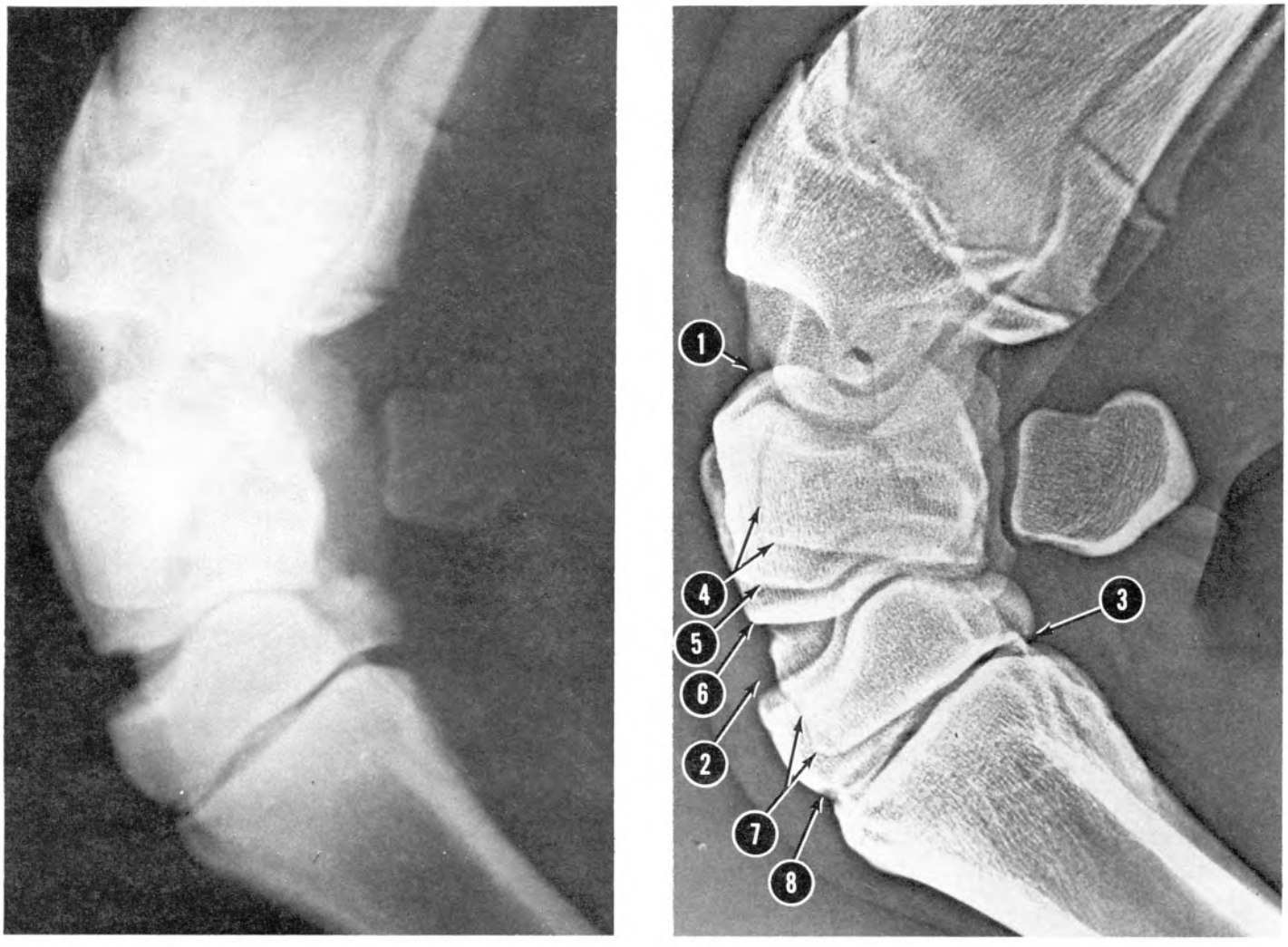

A. Radiograph

B. Xeroradiograph

Figure 3

Flexed Lateromedial View of the Left Carpus

This flexed position shows that the antebrachiocarpal joint (1) and the middle carpal joint (2) have considerable mobility in comparison to the carpometacarpal articulations (3) which are relatively immobile. The ulnar (4), intermediate (5), and radial (6) carpal bones produce superimposed shadows which are separable along their distal and dorsal borders. In this position the fourth carpal bone (7) is rocked away from the metacarpal bone to produce a wedge-shaped deficit which is filled in by C2+3 (8).

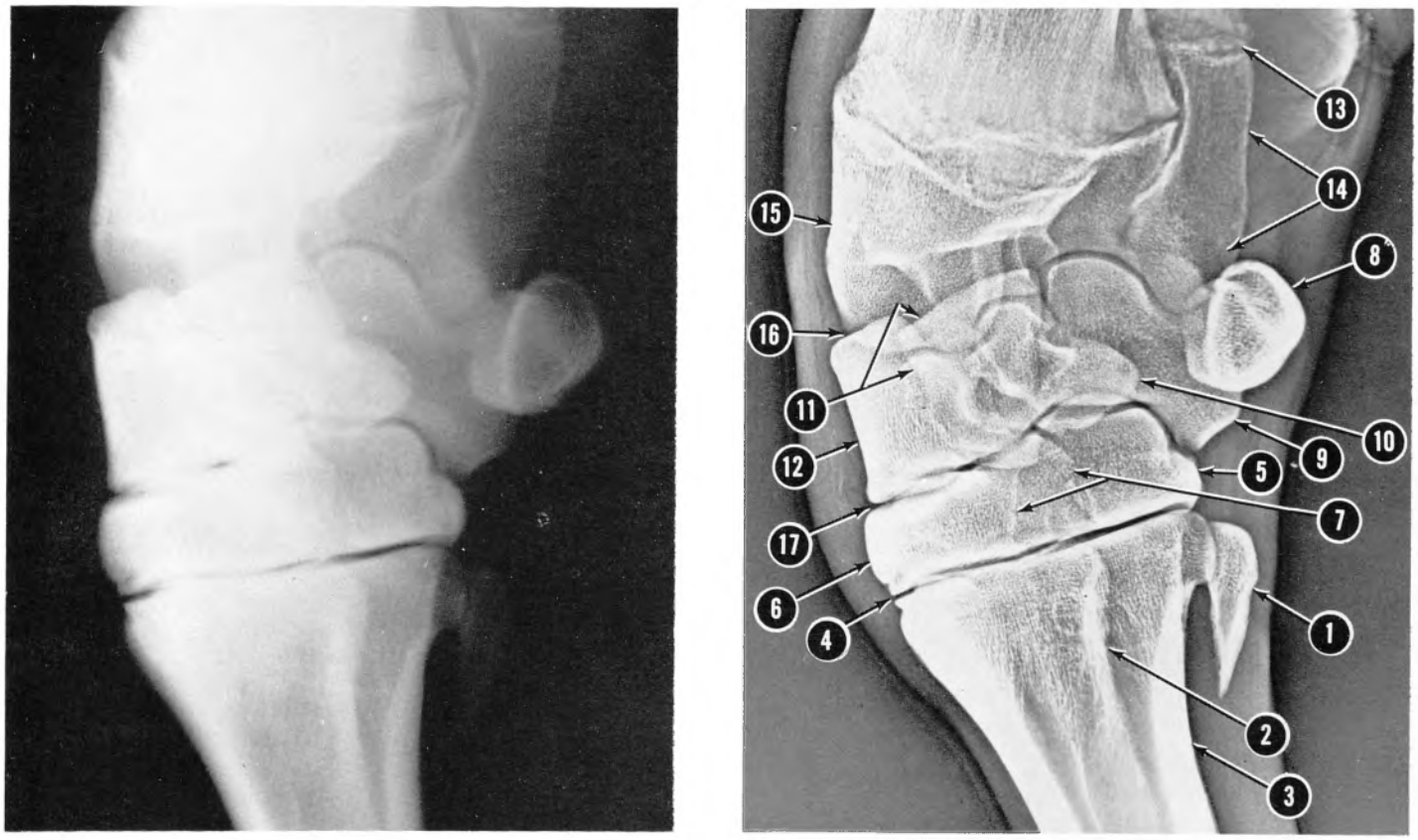

A. Radiograph

B. Xeroradiograph

Figure 4

Dorsopalmar Medial Oblique (APMO) View of the Left Carpus

The fifth metacarpal bone (1) and its articulation with Mc4 are well isolated in this view. In Mc3+4, the tangentially-struck palmar border of the third metacarpal component (2) is superimposed on the fourth metacarpal component (3). The nearly planar nature of the carpometacarpal joints (4) is well illustrated in this view. Even though the fourth carpal bone (5) is partially superimposed on C2+3 (6), the superimposed area (7) does not appear markedly more dense radiographically because about the same thickness of bone is present in the superimposed area as in adjacent areas. The accessory carpal bone (8) appears especially dense because in this perspective it is viewed nearly end-on. The palmar process of the ulnar carpal bone (9) is well isolated and most of the bone is easily defined except for the part superimposed on the lateral palmar process of the intermediate carpal bone (10). Some borders of the intermediate carpal bone are easily defined (11) while others are obscured. The dorsomedial aspect of the radial carpal bone is isolated (12). The distal physis of the ulna (13) and the ulnar styloid process (14) are also well defined. The distal epiphysis of the radius (15) is partially superimposed on the radial, intermediate, and ulnar carpal bones. A skeletal specimen is very helpful in identifying the various overlapping densities along the planes of the antebrachiocarpal (16) and middle carpal (17) joints.

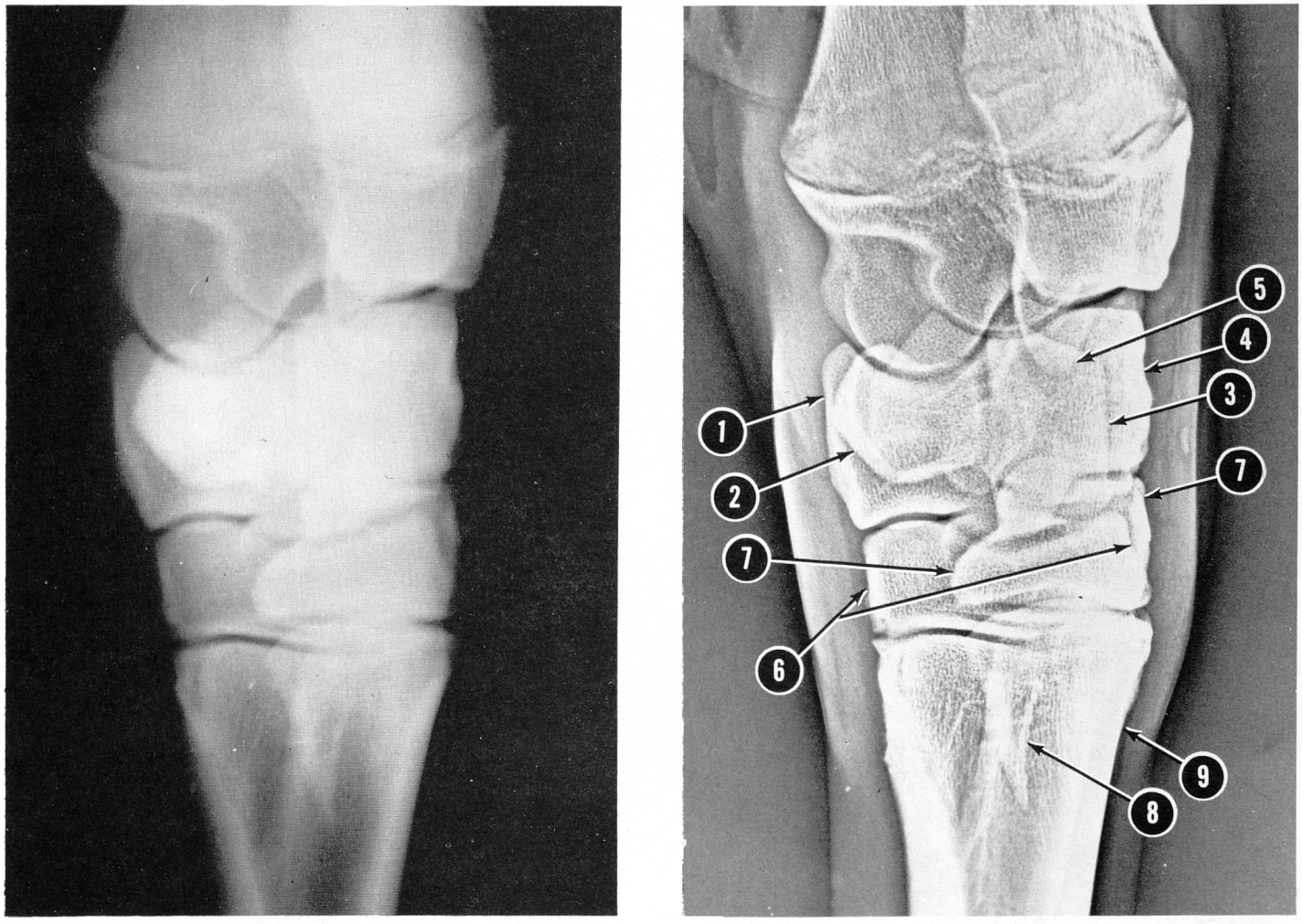

A. Radiograph

B. Xeroradiograph

Figure 5

Dorsopalmar Lateral Oblique (APLO) View of the Left Carpus

This perspective superimposes the shadows of the radial carpal bone (1) and the accessory carpal bone (2). The intermediate carpal bone (3) is superimposed primarily on the ulnar carpal bone (4). Note the distal extent of the ulnar styloid process (5). The image of C2+3 (6) extends across the superimposed fourth carpal bone (7), and the image of the fifth metacarpal bone (8) is centered on Mc3+4 (9).

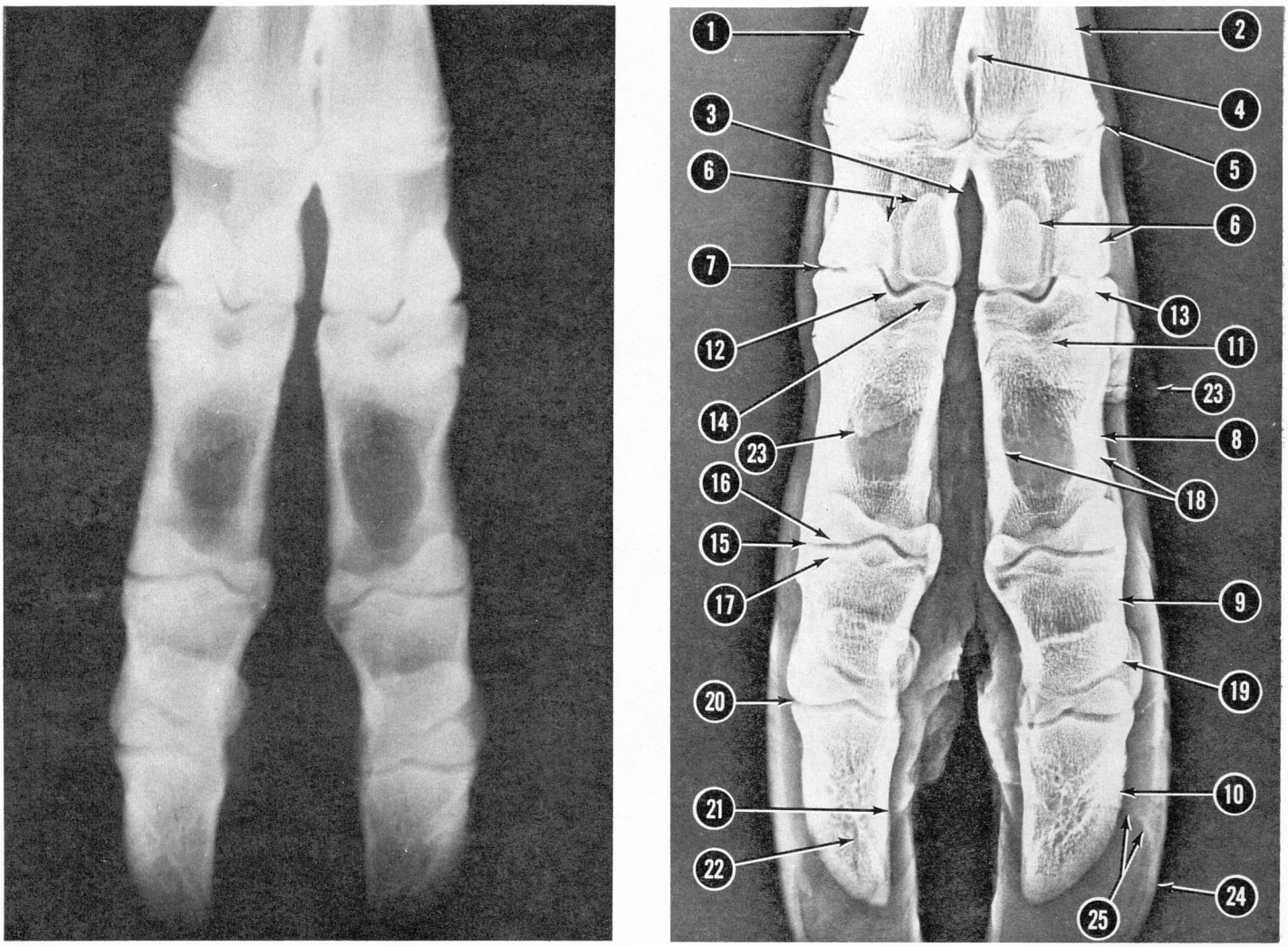

A. Radiograph *B. Xeroradiograph*

Figure 6

Dorsopalmar (AP) View of the Left Digits

The separate origin of the third (1) and fourth (2) components of Mc3+4 are particularly evident at the distal end where they remain separated by the intertrochlear notch (3). The distal metacarpal canal (4) joining the dorsal and palmar longitudinal grooves is evident proximal to the intertrochlear notch. The distal physis of Mc3+4 is still prominent in this young animal (5). The paired proximal sesamoid bones (6) associated with each digit are located proximal to the palmar aspects of the metacarpophalangeal joints (7). Within each digit the proximal phalanx (8) is considerably longer than the middle phalanx (9) or the distal phalanx (10). Physes separating the base and body of each proximal phalanx are faintly evident (11). Sagittal ridges on the heads of Mc3+4 articulate with corresponding grooves in the bases of the proximal phalanges (12). These grooves divide the base of each proximal phalanx into two areas with the abaxial one (13) extending further proximally than the axial one (14). A similar uneven division occurs at the proximal interphalangeal joint (15) involving the head of the proximal phalanx (16) and the base of the middle phalanx (17). The axial and abaxial borders of the body of each proximal phalanx appear particularly radiodense (18) because of the presence of palmar ridges for the attachment of the oblique sesamoidean ligaments. The single distal sesamoid bone (19) of each digit is located at the proximal, palmar aspect of the distal interphalangeal joint (20) and is largely superimposed on the middle phalanx. The distal phalanges have four surfaces: an articular surface, an axial surface (21), a solar (palmar) surface and a parietal (dorsal) surface. Note the numerous vascular channels and foramina in the distal phalanges (22). The distal aspects of the vestigial second and fifth digits (23) are largely superimposed over the proximal phalanges. These vestigial digits (dewclaws) typically contain some rudimentary phalanges (Fig 7/1 and 2). The outline of the hoof wall is sharply delineated by the xeroradiograph (24) but is only faintly visible in the radiograph. The junctions of the soles of the hooves with the bulbs of the heels are also faintly defined (25).

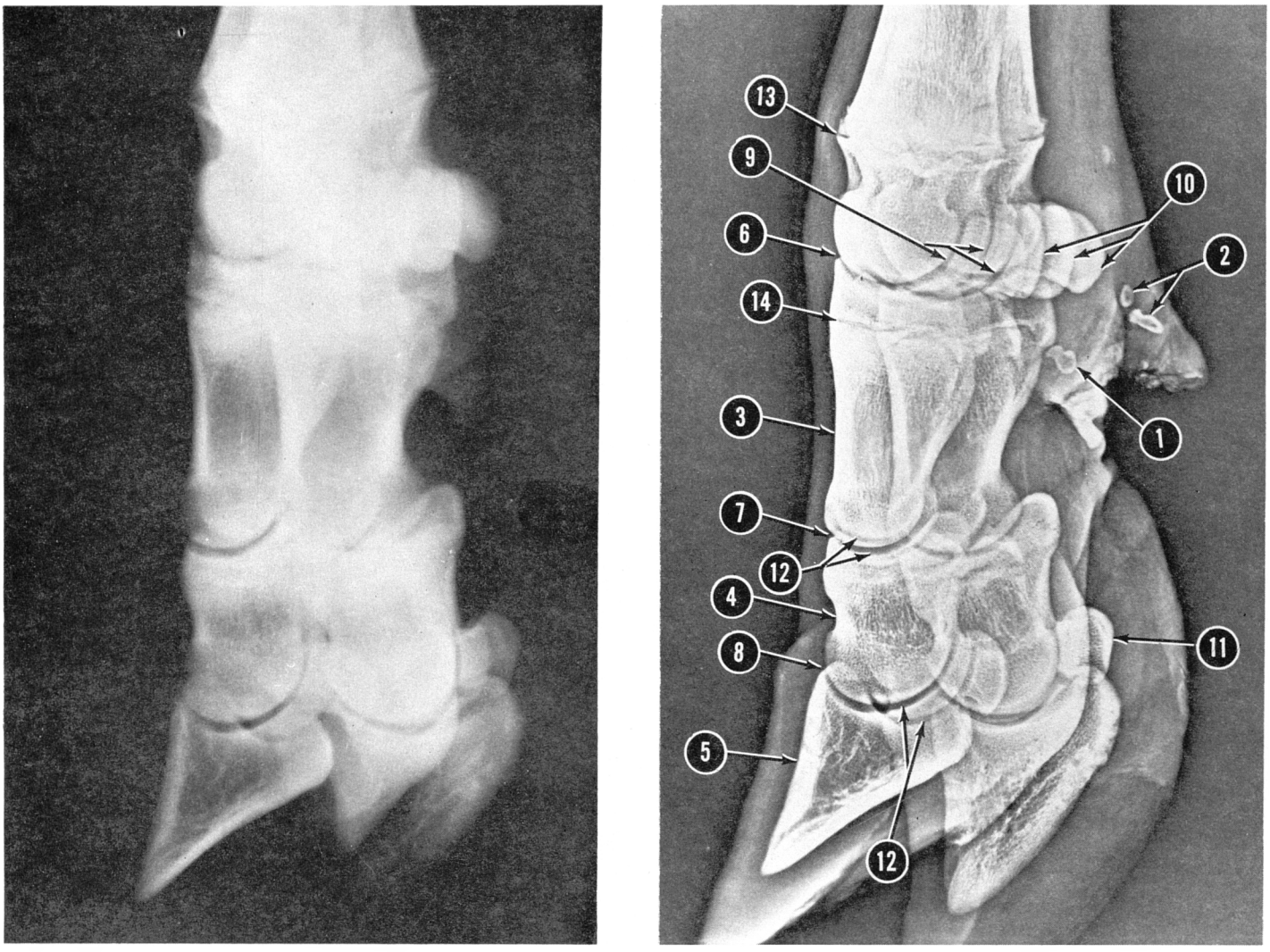

A. Radiograph *B. Xeroradiograph*

Figure 7

Dorsopalmar Medial Oblique (APMO) View of the Left Digits

Rudimentary phalanges in the second (1) and fifth (2) digits (medial and lateral dewclaws) are obvious in the xeroradiograph but difficult to delineate in the radiograph. The proximal (3), middle (4), and distal (5) phalanges of the third digit appear dorsal to those of the fourth digit because of the oblique positioning. The metacarpophalangeal joint (6), proximal interphalangeal joint (7), and distal interphalangeal joint (8) of each digit are easily distinguished although the heads of Mc3+4 and their sagittal ridges (9), and the proximal sesamoid bones (10) cast confusing shadows at the metacarpophalangeal joints. The paired proximal sesamoids of each digit articulate primarily with the head of the metacarpal bone but also with each other and with the proximal phalanx. Similarly the distal sesamoid bone (11) of each digit articulates primarily with the middle phalanx but also with the distal phalanx. The paired imaging at the proximal and distal interphalangeal joints (12) is caused by the curvature of the articular surfaces. The physes of Mc3+4 (13) and the proximal phalanges (14) can be distinguished.

Dorsopalmar Lateral Oblique (APLO) Radiograph of the Left Digits

This oblique view demonstrates the same anatomical features illustrated by the APMO view because of the symmetry of the digits. However, it does isolate the opposite borders of the various bones and is therefore clinically useful to visualize lesions in specific areas. In this view the fourth digit (1) appears dorsal to the third digit (2) and the defined borders of the phalanges are the dorsolateral (3) and palmaromedial (4) borders. In figure 7 (APMO view) the defined borders of the phalanges are the dorsomedial and palmarolateral borders.

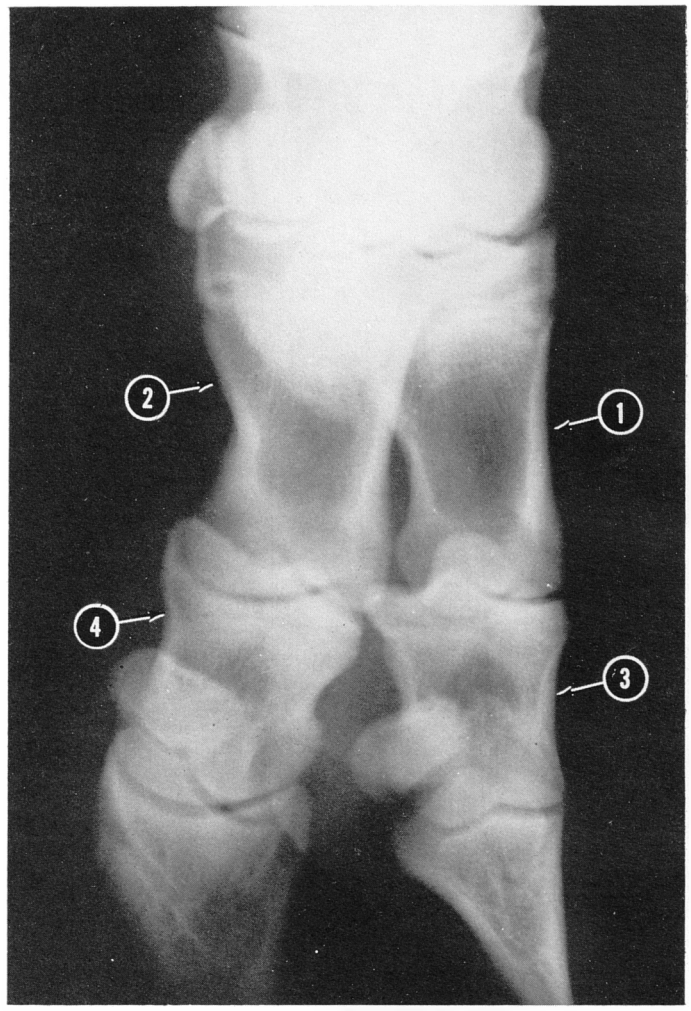

Figure 8